Role of Threonine 101 on the Stability of the Heme Active Site of Cytochrome P450cam: Multiwavelength Circular Dichroism Studies†

Soumen Kanti Manna and Shyamalava Mazumdar*

Department of Chemical Sciences, Tata Institute of Fundamental Research, Homi Bhabha Road, Colaba, Mumbai 400005, India

Received April 30, 2006; Revised Manuscript Received July 31, 2006

ABSTRACT: The role of the threonine 101 residue that resides close to the heme propionic acid side chain of cytochrome P450cam on the conformational properties of the active site of the enzyme has been investigated by circular dichroism (CD) spectroscopy. Site-specific mutation of the threonine by valine has been carried out that does not affect the size of the residue but significantly alters the hydropathy index. The T101V mutant of cytochrome P450cam showed distinct differences in the CD spectra near the heme region, indicating a subtle effect of the mutation on the properties of the heme active site. Thermal stabilities of the mutant and wild-type enzyme have been studied by temperature dependence of the ellipticity (intensity of the CD band) in the far-UV region for the secondary structure and at different wavelengths in the visible region that arise from the heme moiety for the tertiary structure around the prosthetic group. The thermal unfolding data from variations of the CD intensity at different wavelengths were analyzed using a generalized multistep unfolding model, and two distinct equilibrium intermediate conformational states of the enzyme were identified. The mutation of the T101 residue by valine was found to decrease the thermal stability of both the intermediates in the presence of the substrate. On the other hand, this mutation had no apparent effect on the thermal stability of the enzyme in the absence of the substrate. These results suggested that the threonine residue stabilizes the protein cavity around the heme center in the case of the substrate-bound species, possibly by hydrogen bonding with one of the propionate side chains of the heme moiety. Such hydrogen bonding of the heme propionate with threonine is absent in the substrate-free form of the enzyme.

The biological function and stability of a metalloenzyme depend upon subtle conformational properties of the residues in the active site and their interactions with the metal ion or the prosthetic group.

Cytochrome P450 represents a large superfamily of heme-containing mono-oxygenases (*1*). These metalloenzymes are involved in a vast range of biotransformations, including drug metabolism, xenobiotic degradadation, steroid biosynthesis, etc. (*1*−*3*). Most of these enzymes show high regio- and/or stereoselectivity in the catalysis and, hence, have attracted a lot of interest in recent years (*1*, *4*−*6*). The cytochrome P450 from *Pseudomonus putida* (P450cam)[1] is a very well-characterized member of this superfamily of enzymes. It catalyzes the regio- and stereospecific hydroxylation of its natural substrate (1*R*)-camphor to 5-*exo*-hydroxy-camphor (*7*). A great deal of effort is being made to achieve regio- and stereoselective oxygenation of important unnatural substrates (*7*−*14*) by suitably engineered P450cam mutants. It has thus become important to understand the role of the active-site components in substrate recognition, reactivity, and stability of the enzyme.

There are several residues of the enzyme that are invariant among many members of the family, while there are some amino acids near the active site that are found only in P450cam and might have structural or functional roles specific to this particular enzyme. The substrate-binding pocket in the active site of P450cam (*15*) consists mostly of hydrophobic residues (viz., F87, F98, V247, V295, V396, etc.), which stabilize the substrate through van der Waals interactions. These residues are thus important in modulating substrate specificity. There are a few polar residues (viz., Y96, T101, T185, T252, D251, etc.) around the active site as well, some of which have been shown to play important roles in the function of the enzyme. The side chain of Y96 forms a hydrogen bond with the carbonyl group of camphor and, thus, is known to regulate substrate binding (*7*). D251 has been shown to be involved in the proton delivery channel and, thus, plays a key role (*16*−*18*) in the catalytic cycle of the enzyme.

The active site contains three threonine residues, namely, T252, T185, and T101, in cytochrome P450cam. The threonine residues in proteins have been suggested (*19*, *20*) to participate in proton transfer or hydrogen-bonding interactions because of the presence of the alcoholic −OH group in the amino acid. On the other hand, the $-CH_3$ group in threonine may also provide hydrophobic effects to the surroundings. T252 has been shown to be important in

†This work was supported by the Tata Institute of Fundamental Research, Mumbai, India.

* To whom correspondence should be addressed. E-mail: shyamal@tifr.res.in. Telephone: 091-22-22782363. Fax: 091-22-22804610. Home page: http://www.tifr.res.in/∼shyamal.

[1] Abbreviations: P450cam, cytochrome P450cam, CYP101, EC 1.14.15.1; CD, circular dichroism; DSC, differential scanning calorimetry; PDB, Research Collaboratory for Structural Bioinformatics (RCSB) Protein Data Bank, http://www.rcsb.org/pdb/; WT, wild type; T101V, threonine 101 to valine mutant of cytochrome P450cam.

10.1021/bi060848l CCC: $33.50
Published on Web 10/03/2006

oxygen activation and serves to prevent "*uncoupling or slips*" in the catalytic reaction (*16*, *17*, *20*−*22*). T185 is a part of the substrate-binding pocket and directly interacts with the substrate, and mutation of this residue has been shown to modulate substrate binding (*9*, *23*, *24*) to the enzyme. T101 is also a part of the substrate-binding pocket and placed very close the heme (*7*) at the loop between the B′ and C helices. The T101 residue has earlier been mutated to methionine, leucine, and isoleucine for catalyzing smaller hydrocarbons and analogues (*7*, *11*, *13*, *14*, *23*, *25*). These mutations of T101 by bulky amino acids decrease the size of the distal pocket of the heme and, thus, enable binding of smaller substrates. These mutations were also shown to decrease the camphor-binding constant to the mutant enzymes and increase the catalytic activity of the mutant for smaller substrates. There has however been no detailed biophysical study reported on the effects of such mutations on the structure and stability of the enzyme. The T101 residue resides close to the propionate side chains in the distal side of the heme and could potentially have some role in the stability of the protein pocket around the heme moiety. To understand the role of the threonine 101 residue on the stability and substrate binding to the enzyme, we have investigated the effects of the replacement of the threonine by valine at this site, in which the −OH group of threonine is replaced by $-CH_3$ of valine in the mutant. Threonine and valine have almost the same size; hence, this mutation of threonine by valine is not likely to change the size of the protein pocket in the active site and, thereby, would enable us to investigate any possible structural role of T101, especially that of the −OH group of this residue in the enzyme. The effects of this mutation on the structure, substrate binding, and stability of the protein were investigated using UV−vis absorption spectroscopy, circular dichroism (CD) spectroscopy, and differential scanning calorimetry (DSC). Analysis of these results, in conjunction with the reported X-ray crystal structures of P450cam, allowed us to understand the role of the T101 residue in the active site of the enzyme.

MATERIALS AND METHODS

Restriction enzymes and buffers for molecular biology works were obtained from New England Biolabs. DEAE-Sepharose, Q-sepharose, and Sephadex G-25 coloumns were from Pharmacia Biotech. General reagents and (1*R*)-camphor were from Sigma. UV−vis absorption spectra were measured on a Shimadzu(UV-2100) spectrophotometer coupled with a Peltier-controlled thermostated cell holder. CD spectra were measured on a JASCO J-810 spectropolarimeter equipped with a Peltier cell temperature controller (±0.2 °C).

Mutation, Expression, and Purification. The $pCHC_1$ plasmid, encoding cytochrome P450cam C334A (*26*), was a kind gift from Prof. L.-L. Wong (University of Oxford, Oxford, U.K.). Site-directed mutagenesis was carried out using the Quikchange site-directed mutagenesis kit (Stratagene). The forward and reverse primers used for the threonine 101 to valine mutant of cytochrome P450cam (T101V) mutation were 5′-CTTCATTCCCgtaTCGATGGATCCG-3′ and 3′-GAAGTAAGGGcatAGCTACCTAGGC-5′, respectively, obtained from GENEI (Bangalore, India). These primers introduced a unique *Cla*I restriction site into the 323 bp position of the *camC* gene along with a T101V mutation (shown in small letters). Polymerase chain reaction (PCR) amplification of the mutant gene was carried out on a PTC-2000 Peltier thermocycler (MJ Research, Waltham, MA). Plasmids were isolated from the colonies obtained upon transforming the PCR product into XL1-blue Supercompetent cells (Stratagene). Both the wild-type (WT) (i.e., C334A) and T101V (i.e., C334A, T101V double mutant) cytochrome P450cam were expressed using *Escherichia coli* BL21-DE3 cells. The proteins were expressed and purified using a slight modification of the reported method (*26*). Purified protein, with $A_{390}/A_{280} \geq 1.5$, was concentrated and stored in small aliquots in 40% (v/v) glycerol at −30 °C. The protein solutions were passed through a pre-equilibrated Sephadex G-25 column (pre-packed Amersham Pharmacia PD-10) to remove glycerol before each experiment.

UV−Vis Spectroscopy. All spectra were recorded at 20 °C unless mentioned otherwise. The substrate-free form was obtained by passing the protein twice through the G-25 column, pre-equilibrated, and subsequently eluted with 50 mM Tris base (pH 7.4). Substrate-bound protein was obtained in the presence of 1 mM camphor along with 100 mM KCl. Extinction coefficients of the T101V mutant were determined by the *pyridine hemochrome method* following the standard protocol (*27*). The extinction coefficients for the camphor-bound WT and mutant enzyme at 391 nm were 102 and 108 mM^{-1} cm^{-1}, respectively. These values were found to be 119 and 123 mM^{-1} cm^{-1}, respectively, for the camphor-free forms of the WT and mutant enzyme at 417 nm. The camphor-binding constant was determined by titrating the substrate-free enzyme with camphor in the presence of 100 mM KCl, and data were analyzed by the reported method (*28*).

CD Spectroscopy. CD spectra for the secondary-structure region (195−260 nm) were recorded using 3 μM enzyme in a quartz cuvette of 1 mm path length. The temperature dependence of the secondary structure was studied by monitoring the CD signal at 221 nm in the presence of 100 mM KCl, with or without 1 mM (1*R*)-camphor. The CD spectra in the tertiary-structure region (260−450 and 450−650 nm) were recorded using 15−20 μM enzyme in a quartz cuvette of 1 cm path length. The temperature dependence of the CD signal of the substrate-free protein was monitored at 410, 408, and 580 nm for the WT and T101V. The temperature dependence of the CD signal for the camphor-bound form was monitored at 389 and 538 nm for both the WT and T101V mutant. All of the experiments were done with a freshly prepared sample in 50 mM Tris base (pH 7.4). The temperature ranges monitored were 20−85 °C. The temperature scans were performed with a data pitch of 0.2 °C along with the simultaneous recording of the spectra at an interval of 5 °C.

Data Analysis. The thermal unfolding data, monitored at different wavelengths, with distinct pre- and post-transition regions were analyzed using a simple two-state equilibrium model (*29*) between native (N) and unfolded (U) conformations (N ⇌ U) to determine apparent T_m (T_m^{app}) values for the unfolding transition.

The data were also analyzed using a multiple conformational equilibrium model

$$C_1 \rightleftharpoons C_2 \cdots C_n \rightleftharpoons C_{n+1} \quad (1)$$

where C_1 represents the native conformation (N), C_2, C_3, and

C_n are intermediate conformations, and C_{n+1} is the final unfolded conformation of the enzyme (U).

The fraction of the unfolded (apparent) form was obtained from the observable (O^λ) (e.g., intensity of the CD signal at a given wavelength) and from the initial (O_0^λ) and final (O_∞^λ) values at the same wavelength λ, as

$$f_u^{app} = \frac{O_0^\lambda - O_{obs}^\lambda}{O_0^\lambda - O_\infty^\lambda} \quad (2)$$

The variation of f_u^{app} with temperature at different wavelengths was analyzed using the generalized equation (*30*)

$$f_u^{app} = \frac{\sum_{i=1}^{n+1}\left\{\Delta x_i^\lambda \prod_{j=1}^{i} e^{-\Delta G^T_{j/RT}}\right\}}{1 + \sum_{i=1}^{n+1}\left\{\prod_{j=1}^{i} e^{-\Delta G^T_{j/RT}}\right\}} \quad (3)$$

where Δx_i^λ is the weighted difference in spectral characteristics (e.g., molar ellipticity, extinction coefficient, etc.) of the *i*th conformation with respect to the native conformation at wavelength λ. ΔG_j^T is the standard free energy of unfolding at temperature T for the *j*th conformation.

The ΔG_j^T (given as $\Delta H_j^T - T\Delta S_j^T$) is related to the standard enthalpy change ($\Delta H_{T_{mj}}$) at the transition midpoint temperature (T_{mj}) for the *j*th conformation as follows:

$$\Delta H_j^T = \Delta H_{T_{mj}} + \Delta C_{pj}(T - T_{mj})$$

$$\Delta S_j^T = \frac{\Delta H_{T_{mj}}}{T_{mj}} + \Delta C_{pj} \ln(T/T_{mj})$$

$$\Delta G_j^T = (\Delta H_{T_{mj}} - \Delta C_{pj} T_{mj}) + T(\Delta C_{pj} - \Delta H_{T_{mj}}/T_{mj}) - T\Delta C_{pj} \ln(T/T_{mj}) \quad (4)$$

Putting the value of ΔG_j^T from eq 4 into eq 3 and nonlinear least-square fit of the CD data at different wavelengths to eq 3 were used to determine the values of thermodynamic parameters associated with the thermal unfolding of the protein.

DSC. The DSC was performed using a VP-DSC microcalorimeter (MicroCal LLC, Northampton, MA). The DSC experiments were performed with 1.8 mg/mL (35.8 μM) WT and 2.1 mg/mL (44.2 μM) T101V protein in 50 mM Tris (pH 7.4) buffer in the presence of 1 mM camphor along with 100 mM KCl. The temperature range of scans was 10−80 °C at a scan rate of 60 °C/h. The raw experimental data were corrected by substracting the baseline to remove any effects from changes in the molar heat capacity before and after the transition.

RESULTS AND DISCUSSION

The UV−vis absorption spectra of the WT and T101V mutant of cytochrome P450cam are identical to each other (Figure 1). However, there is a small decrease (~5%) in the relative intensities of the visible bands (500−650 nm region) with respect to the Soret absorption in the mutant compared to that in the WT enzyme both in the absence and presence of camphor. Such subtle differences in the relative absorbances of the visible bands compared to the Soret band of the heme might indicate small changes in the heme in-plane interactions in the active-site pocket of the enzyme upon mutation.

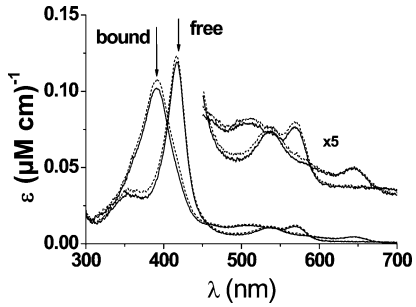

FIGURE 1: UV−vis spectra of camphor-free and camphor-bound forms of the WT (—) and T101V mutant (- - -) of cytochrome P450cam. The visible bands are expanded 5 times.

To evaluate the effect of mutation on the overall binding of camphor to the enzyme, we determined the apparent binding constants (K_b^{app}) of camphor to the WT and mutant enzyme by the UV−vis titration method as described earlier (*28*) at 20 °C. The spectral dissociation constant (K_s) for (1*R*)-camphor to the WT cytochrome P450cam was found to be 1.92 ± 0.2 μM (K_b^{app} = 0.52 ± 0.06 μM^{-1}), which agreed with an earlier paper (*28*). The camphor-binding constant (K_b^{app}) for the T101V mutant was found to be almost the same (K_b^{app} = 0.48 ± 0.06 μM^{-1}, K_s = 2.1 ± 0.3 μM) as that in the case of the WT enzyme.

The above results thus suggest that the mutation of the threonine 101 residue with valine possibly has only a small effect on the electronic property of the heme. Moreover, the results also suggest that this mutation does not directly affect the binding of the camphor and the substrate−protein interactions that consist of hydrogen bonding of camphor with Y96 and hydrophobic interactions with other active-site residues. Earlier studies (*25*) on the T101M mutant of cytochrome P450cam reported a 24-fold decrease in the camphor-binding constant in the mutant (T101M) compared to that in the WT enzyme, indicating that methionine being a bulkier residue possibly causes steric crowding near the distal pocket of heme, leading to a decrease in the substrate-binding affinity of the enzyme. On the other hand, the replacement of the −OH group of threonine 101 by $-CH_3$ in the T101V mutant of the enzyme would not impart any extra steric interaction to the active site and, hence, does not affect the camphor-binding constant to the enzyme. However, the T101V mutation is likely to cause changes in the hydropathy (from a hydropathy index −0.7 of threonine to +4.2 of valine) in the vicinity of the heme residue and could have a subtle effect on the tertiary interactions at the active-site pocket of the enzyme.

To investigate the effect of the mutation on the conformational properties of the enzyme, we have carried out detailed multiple-wavelength CD studies of the WT and T101V mutant cytochrome P450cam. The far-UV CD bands (190−260 nm) of the protein arise because of regular asymmetric structures, such as α helix, β sheet, random coils, etc., around the peptide chromophore. The CD signal in this region provides information on these secondary-structural components of the protein. Parts A and B of Figure 2 show

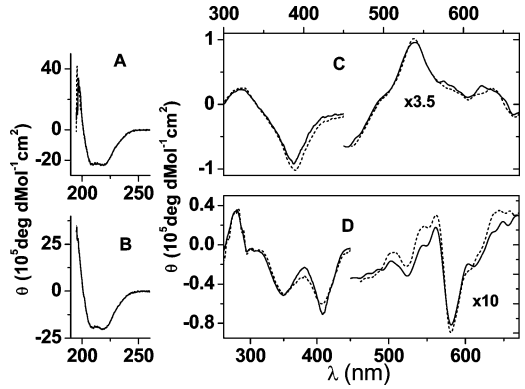

FIGURE 2: Far-UV CD and visible CD spectra of substrate-bound forms (A and C) and substrate-free forms (B and D) of the WT (—) and T101V mutant (- - -) of cytochrome P450cam.

the CD spectra in a 195−260 nm region, respectively, for camphor-bound and free forms of the WT and T101V cytochrome P450cam. The results show that the mutation of the threonine residue has no effect on the secondary structure of the protein. The analysis of the secondary structure (*31*) reveals that the α-helical content of the enzyme in the presence and absence of camphor is 46% and 40%, respectively, which is in agreement with those reported earlier (*15*, *32*).

The CD spectrum in the near-UV region (260−300 nm) arises mainly because of tertiary interactions near the aromatic residues, such as phenylalanine, tyrosine, tryptophan, etc., in the protein. These residues are widely distributed over the structure of cytochrome P450cam, and hence, the near-UV CD of the enzyme would provide information of the overall tertiary structure of the enzyme. The CD spectrum of the enzyme in the near UV region was found to be almost the same in the T101V mutant and WT enzyme, indicating that the overall tertiary structure of the enzyme was possibly not altered upon mutation. However, because the CD signals in this spectral region are weak, any small localized changes in the tertiary structure could not be detected from CD in this region.

The heme absorption bands in the protein give rise to the heme CD in the visible region (300−675 nm) because of anisotropic interactions between the aromatic amino acid side chains and the heme chromophore in the protein cavity. The heme CD thus contains information about the relative spatial arrangements of the heme and the aromatic side chains in the tertiary structure of the protein. The overall pattern of the visible CD spectra of the WT and T101V mutant of cytochrome P450cam was found to remain unchanged (Figure 2). However, close inspection of the results indicated that there are indeed small but distinct differences in the peak positions as well as in the intensities of the CD bands between the WT and mutant enzymes as shown in parts C and D of Figure 2.

The camphor-bound form of the T101V mutant (Figure 2C) showed a small shift (∼2 nm) in the maxima in the heme CD spectrum in the Soret region compared to those of the WT enzyme. More notably, the heme CD band that is characteristic of a high-spin five-coordinated geometry of the heme, with a maximum at 623 nm in the WT enzyme, was shifted to 635 nm in the T101V mutant in the presence of camphor.

The Soret and δ bands in the heme CD spectrum of the enzyme in the absence of the substrate appear, respectively, at 409 and 351 nm for the WT and at 406 and 352 nm for the T101V mutant of the enzyme (Figure 2D). The ratio of these two peaks (Soret/δ) was found to be more in the WT (∼1.4) enzyme compared to that in the T101V mutant (∼1.1). This ratio has earlier been shown to be positively correlated (*33*) to the extent of polarity or hydrogen bonding at the active site of the P450 enzyme. Thus, a decrease in the ratio of intensities of Soret/δ CD bands in the T101V mutant reflects a decrease in polarity and/or loss of hydrogen bonding at the active site because of the mutation in the absence of the substrate. Figure 2D also shows that, unlike in the case of the substrate-bound cytochrome P450cam, the CD peak positions in the visible region in the substrate-free enzyme remained unchanged upon mutation, although the intensities were slightly higher in the T101V mutant compared to that in the WT cytochrome P450cam.

A comparison of the CD spectra of the enzyme and its mutant at different wavelength regions thus shows that, although the secondary structure of the enzyme was not affected by the T101V mutation, there was indeed a distinct change in the tertiary structure around the heme pocket in the mutant compared to that in the WT enzyme. Moreover, the conformational change because of the mutation was more significant in the case of the substrate-bound T101V mutant, which showed a ∼12 nm shift in the visible CD band that appears at 623 nm in the WT enzyme.

Unfolding of the Enzyme. Equilibrium unfolding of the WT as well as the T101V mutant cytochrome P450cam was carried out to determine the effect of the mutation at the T101 site on the stability of the enzyme. The addition of a chemical denaturant such as urea or an increase in the temperature causes a steady decrease in the absorbance of the heme because of the unfolding of the enzyme (*30*). The unfolding of the enzyme was a complex and multistep process as reported by us earlier (*30*). The neutral denaturant, urea, drastically perturbs the structure of the enzyme and, thus, would not be able to identify any subtle effect of the threonine 101 residue on the stability of the enzyme. Unlike the chemical unfolding, thermal unfolding of the enzyme takes place by a increase in the internal energy of the system upon thermal excitation and would be able to identify any changes even in weak interactions (such as hydrogen bonding) between residues upon mutation. The effects of the thermal excitation on the secondary as well as tertiary structures around the heme were hence investigated by CD spectroscopy of the WT and mutant enzyme. The temperature dependence of the CD signal in the far-UV region (190−260 nm) would give information about the thermal unfolding mainly of the secondary-structural elements of the protein. The changes in the CD signal in the visible region, on the other hand, will be dependent not only on changes in the secondary structure but also on changes in the tertiary-structural elements that form the typical spatial organization of the protein cavity around the heme center. Moreover, the heme CD at different wavelengths could also have different contributions from a particular tertiary-structural element of the heme cavity as reported earlier in the case of cytochrome *c* (*34*, *35*). Thus, temperature dependence of the visible CD bands at different wavelengths would give information on the thermostability of the tertiary-structural elements of the heme pocket, including the factors that hold the heme in its native position inside the protein matrix, i.e., axial ligation

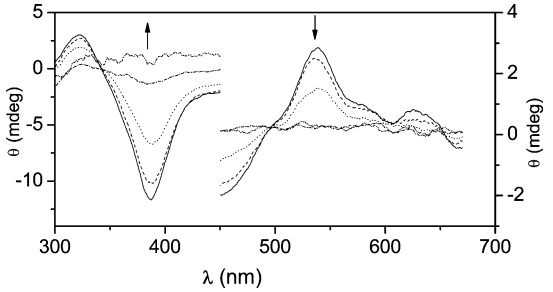

FIGURE 3: Typical temperature variation of the visible CD spectra of cytochrome P450cam in the presence of camphor.

Table 1: Apparent T_m Values for Thermal Unfolding of the WT and T101V Mutant of Cytochrome P450cam Determined from CD at Different Wavelengths

spectral region	T_m^{app} (K) camphor bound		T_m^{app} (K) camphor free	
	WT	T101V	WT	T101V
far UV[a]	333.2 ± 0.5	333.4 ± 0.5	323.3 ± 0.5	323.8 ± 0.5
visible I[b]	334 ± 0.5	330.5 ± .5	321.2 ± 0.5	320 ± 0.5
visible II[c]	333.7 ± .5	330.6 ± 0.5	317.5 ± 0.5	316.3 ± 0.5

[a] Far-UV CD was monitored at 221 nm. [b] Visible I corresponds to the CD band at 389 and 410 nm, respectively, in the presence and absence of camphor. [c] Visible II corresponds to the CD band at 538 and 580 nm, respectively, in the presence and absence of camphor.

of the metal ion to the protein, van der Waals interactions, hydrogen bonding, ion-pair formation with heme-propionate side chains, etc. The effect of the mutation on the thermal stability of the enzyme was also studied by DSC that measures the overall heat changes associated with the thermal unfolding of the protein.

To probe the effect of the mutation of the threonine 101 residue with valine on the thermal stability of different tertiary-structural elements of the protein, we monitored the thermal unfolding of the enzyme by CD at different wavelengths corresponding to different CD bands. All of the CD bands of the enzyme decreased upon an increase in the temperature of the protein solution, indicating thermal unfolding of the structure of the protein. The thermal equilibrium at every temperature was ensured by maintaining a slow rate of change in the temperature (1 °C/min), and reversibility of the transition was checked at each temperature as reported earlier (*30*). Figure 3 shows a typical CD spectral variation with temperature. Moreover, the temperature dependence of the CD bands of the enzyme at different wavelengths was found to be slightly different from each other in some cases. This indicated that there might be multiple conformational states involved in the thermal unfolding process that show different effects on the temperature dependence of the CD bands at different wavelengths. The temperature dependence of the CD band at 221 nm predominantly reflected unfolding of the secondary structure of the enzyme. The conformational anisotropy around the heme prosthetic group was monitored at 410 and 580 nm for the camphor-free form and 389 and 538 nm for the camphor-bound form of the enzymes.

The apparent T_m (T_m^{app}) values were determined as the midpoint temperature of the thermal dependence of the CD intensity at different wavelengths and presented in Table 1. The results show that in the case of the camphor-bound enzyme the apparent T_m ($T_m^{app} \approx 333$ K) for the secondary-structure region remains almost the same in the WT and T101V mutant. However, the apparent T_m ($T_m^{app} \approx 333$ K for WT and 330 K for T101V) for the tertiary structure determined from the heme CD at the Soret as well as visible regions decreased by ~3 °C (3 K) in the T101V mutant compared to that in the WT enzyme. These results also indicate that the apparent midpoint temperature was almost the same ($T_m^{app} \approx 333$ K) for the unfolding of the secondary as well as tertiary structure of the WT enzyme in the presence of camphor. This implies that the secondary and tertiary structures of the WT enzyme in the presence of the substrate are "connected" and unfold concurrently (cooperatively), while upon mutation of the threonine 101, such a structural cohesion is lost and the tertiary structure around the heme becomes weaker compared to the secondary structure.

Table 1 also shows that the apparent T_m values (T_m^{app}) for the thermal unfolding of the enzyme in the absence of camphor are smaller than those in the presence of camphor. Moreover, although the secondary structure of the WT enzyme and its mutant unfolds at $T_m^{app} \sim 324$ K, the various tertiary-structural elements that contribute to the heme CD spectrum of the enzyme unfold at a different T_m^{app} (321 and 316 K, respectively, when monitored at 410 and 580 nm CD bands). This indicates that the absence of a substrate not only weakens the secondary structure of the enzyme but also leads to the loss of "connectedness" of various tertiary-structural components around the active site with the secondary structure. It is important to note that, unlike in the case of the substrate-bound enzyme, the mutation of the threonine 101 residue with valine (in T101V mutant) has almost no effect on the thermal stability of the enzyme (Table 1) in the absence of the substrate.

These results suggest that binding of the substrate at the active site of the enzyme possibly introduces certain interactions between the heme and protein matrix, which stabilizes the heme inside the active site. Such an interaction is possibly absent in the case of the T101V mutant (where $-OH$ is replaced by $-CH_3$) enzyme, leading to a decrease in the thermal stability of the heme pocket in the mutant enzyme in the presence of the substrate. Such a stabilization of the heme pocket by threonine is not present in the absence of the substrate; hence, the stability of the T101V mutant is almost the same as that of the WT enzyme in the absence of camphor.

The temperature dependence of the CD intensity was also analyzed using a generalized unfolding model, and data were fit to eq 3 (where ΔG_j^T was expanded as given in eq 4). A simultaneous fit of the temperature-dependent CD (ellipticity) data (about 300 points at each wavelength) at three different wavelengths was performed using a global-fitting routine with the thermodynamic parameters in eqs 3 and 4 shared between different data sets. This gave self-consistent optimized values of the parameter sets. The best fit to the data was ascertained from the R^2 (reduced χ^2) minimizations using Lavenberg−Marquardt and Simplex methods. The goodness of fit was also checked from the randomness of the residual distributions for the fit. The optimum value of n was found to be 3, which indicated the following type of unfolding transition:

$$C_1 \rightleftharpoons C_2 \rightleftharpoons C_3 \rightleftharpoons C_4 \qquad (5)$$

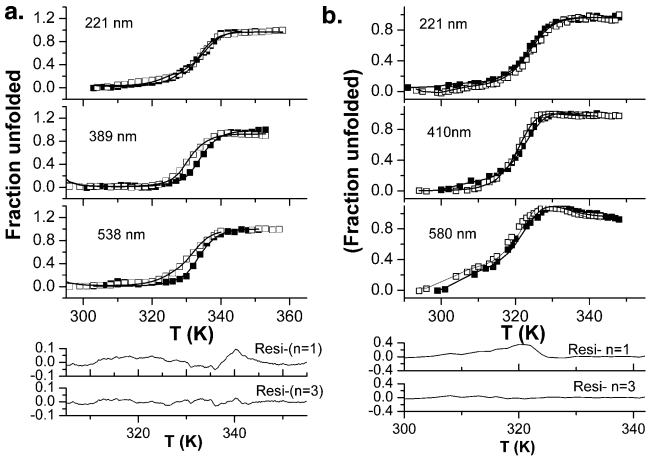

FIGURE 4: (a) Thermal unfolding of the WT (■) and T101V (□) cytochrome P450cam in the presence of camphor. Thermal variations of CD at 221, 389, and 538 nm are converted to the fraction unfolded enzyme. Solid lines through the data are fit to the eq 3. The typical residual distributions for the two-state model (Resi, $n = 1$) and the four-state model (Resi, $n = 3$) are shown in the figure. (b) Thermal unfolding of the WT (■) and T101V (□) cytochrome P450cam in the absence of camphor. Thermal variations of CD at 221, 410, and 580 nm are converted to the fraction unfolded enzyme. Solid lines through the data are fit to the eq 3. The typical residual distributions for the two-state model (Resi, $n = 1$) and the four-state model (Resi, $n = 3$) are shown in the figure.

Table 2: Calculated H_m and T_m Values Obtained from the Fit to the Temperature-Dependent CD Data Using the Multiple Unfolding Steps Model (Eq 3) for Camphor-Bound and Camphor-Free WT and T101V Mutant Cytochrome P450cam

	camphor bound		camphor free	
parameter	WT	T101V	WT	T101V
H_{m1} (kJ)	426 ± 5	424 ± 5	225 ± 10	225 ± 10
H_{m2} (kJ)	166 ± 2	157 ± 2	82 ± 2	80 ± 2
H_{m3} (kJ)	70 ± 3	61 ± 3	20 ± 3	18 ± 3
T_{m1} (K)	335 ± 0.5	335 ± 0.5	327 ± 0.5	327 ± 0.5
T_{m2} (K)	329 ± 0.5	326 ± 0.5	318 ± 0.5	318 ± 0.5
T_{m3} (K)	321 ± 0.5	318 ± 0.5	315 ± 0.5	315 ± 0.5

where C_1 and C_4 respectively correspond to the native (N) and unfolded (U) forms of the enzyme and the thermal unfolding involves two intermediates C_2 and C_3 conformations of the enzyme. Parts a and b of Figure 4 show the variations of the CD intensities of the WT and mutant enzyme with the temperature at different wavelengths, respectively, in the presence and absence of the substrate, along with the fitted curves through the data. The residuals for the fit of the data using eq 3 with $n = 3$ showed a random distribution, while those for a simple two-state equilibrium model ($n = 1$) or for a model with one intermediate state ($n = 2$) showed nonrandom variations. The typical residual distributions for the two-state model ($n = 1$) and the four-state model ($n = 3$) are shown in Figure 4.

Results of the analyses of the data are given in Table 2, which show that, although the apparent T_m (T_m^{app}) determined from temperature dependence at different wavelengths was different (Table 1), temperature dependence of the CD bands at each wavelength indeed reflects all of the three phases associated with the unfolding transition of the enzyme as shown in eq 5. The results further show that the "high-temperature" phase with the highest T_m values ($T_{m1} = 335$ and 327 K) in the presence and absence of the substrate were close to the respective apparent T_m ($T_m^{app} = 333$ and 324 K) values obtained from the temperature variation of the CD band at 221 nm. This midpoint temperature (T_{m1}) corresponds to the unfolding of the secondary structure of the enzyme, and results show that the T101V mutation has no effect on this unfolding phase of the enzyme.

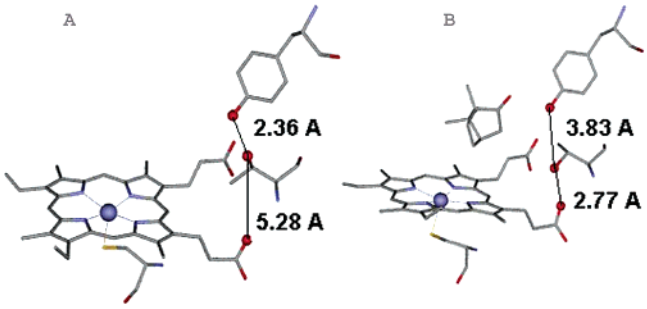

FIGURE 5: Active site of (A) substrate-free (PDB 1PHC) and (B) (1*R*)-camphor-bound (PDB 1DZ4) WT P450cam, showing the orientation of T101 side chain "OG" and its distances from the heme propionate "OD2" and Y96 side chain "O".

The second and third phases possibly correspond to the unfolding of the tertiary-structural components of the enzyme, and the T_m values (T_{m2} and T_{m3}) for these phase transitions were much lower compared to that for the first-phase transition (T_{m1}). Moreover, the T_m values (T_{m2} and T_{m3}) corresponding to the unfolding of the tertiary-structural components around the heme were decreased (by 3 K) upon mutation of the T101 residue by valine in the case of the substrate-bound enzyme. This supports that the threonine residue plays an important role in the stabilization of the tertiary structure around the heme especially in the substrate-bound form of the enzyme. The values of T_{m2} and T_{m3} for the enzyme in the absence of camphor were lower than those in the presence of camphor, further supporting that, analogous to the secondary structure, the substrate also stabilizes the tertiary structure of the enzyme. However, unlike in the case of the substrate-bound enzyme, T_{m2} and T_{m3} in the substrate-free enzyme did not show any significant difference between the WT and mutant enzyme. This suggested that threonine 101 does not have any direct role in the stabilization of the enzyme in the absence of the substrate.

It is important to note that the changes in the stability of the tertiary-structural components that were detected in the temperature dependence of the multiple-wavelength CD data cannot be easily assigned to any specific changes in the structure of the enzyme. The spatial arrangements of aromatic residues around the heme that constitute the observed CD spectrum of the enzyme in the visible region may not belong to a particular structural domain of the protein. Although the T101 residue does not directly contribute to the observation of the heme CD signals, subtle changes in this residue could affect the relative spatial arrangements of some nearby residues that contribute to the CD spectrum of the heme. The decrease in the stability of the tertiary-structural elements around the heme in the T101V mutant enzyme in the presence of the substrate also indicates that the threonine residue might be involved in stabilizing the specific spatial organization of certain residues/moiety in the protein pocket. A comparison of the crystal structures of the camphor-bound and camphor-free cytochrome P450cam (Figure 5, see later) indicated that the −OH group of the threonine residue is

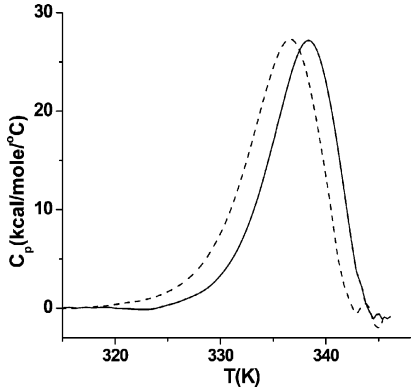

FIGURE 6: Baseline-corrected DSC profile of the camphor-bound WT (—) and T101V mutant (- - -).

indeed closer to a propionic acid group of the heme in the case of the substrate-bound enzyme.

The thermal unfolding of the camphor-bound form was also studied by DSC. Figure 6 shows the baseline-corrected DSC data for thermal unfolding of camphor-bound WT and T101V cytochrome P450cam. The DSC peak shows a small shift from 338.4 K, for the WT, to 336.6 K for the T101V mutant. Earlier differential scanning calorimetric studies (*36*) on the enzyme reported a similar value of the midpoint temperature (336.7 K) for the camphor-bound enzyme, which agreed with the secondary-structure unfolding temperature (335 K) observed in the present work from CD studies (Table 2). The unfolding temperature for the enzyme in the absence of the substrate was earlier (*36*) reported by DSC studies as 326.3 K, which also agrees with the present CD results for unfolding of the secondary structure of the enzyme in the absence of the substrate. Deconvolution of the DSC data upon unfolding of the cyanide complex of cytochrome P450cam was earlier shown to have three phases (*37*), which supports the present results of the temperature dependence of the CD data of the enzyme. The thermal unfolding of the enzyme during DSC studies however was likely to be associated with aggregation of the unfolded protein at high temperatures because the experiments often require a high concentration of the enzyme. This might be the reason for the observation of a slightly higher midpoint temperature in the DSC studies. Moreover, the heat changes associated with the secondary structure were much higher than those with the tertiary structure around the active site. Hence, the contribution of the tertiary structure unfolding to the overall heat change would be very small compared to that for the overall change in the secondary structure and possible subsequent aggregation of the enzyme. Therefore, we did not attempt to deconvolute the DSC data to derive any effects of the T101V mutation on the tertiary-structural changes in the enzyme.

Conformation of the Threonine 101 Residue in the Protein. Earlier studies on microsomal P450 and P450cam suggested the existence of multiple stability components (*30*, *36*−*38*) in the protein. The present results thus indicate that the temperature sensitivity of different CD bands at different wavelengths might actually reflect the thermostability of different components of the tertiary structure. Inspection of the structure of the active site of the camphor-bound enzyme [Protein Data Bank (PDB) 1DZ4] showed that the distance between heme-propionate side-chain oxygen (O2D) and T101 side-chain oxygen (OG) is ∼2.77 Å. This suggests that the −OH group of T101 might be involved in hydrogen bonding with the heme-propionate group (Figure 5). A survey of available high-resolution P450cam structures in the presence of camphor of various species such as the oxygen complex (Fe−O_2, PDB 1DZ8), oxo complex (Fe−O, PDB 1DZ9), ferrous−CO complex (PDB 1A1O), and even the cyanide-bound form (Fe−CN, PDB 1O76) show that the distances between the heme propionate and the −OH of threonine are indeed within hydrogen-bonding length (2.73−3 Å). On the other hand, crystal structures of the enzyme in the absence of the substrate (PDB 1PHC) or in the presence of weak unnatural substrates, such as phenyl imidazole (PDB 1PHD and 1PHF), metyrapone (PDB 1PHG), camphane (PDB 6CPP) etc., show that the distance between the −OH group of T101 and the heme propionate is about 5.3 Å, which is much larger than any possible hydrogen bond. This supports that there is indeed a conformational change of the T101 residue upon binding camphor. The rotation around the C_α−C_β bond of T101 upon binding the substrate could bring the −OH group closer to the heme propionate. Moreover, the crystal structures also show that the −OH group of T101 could form a hydrogen bond with tyrosine 96 in the absence of camphor or in the presence of weak unnatural substrates. Thus, the binding of camphor that involves the interaction of the −OH group of tyrosine 96 with the substrate triggers a conformational change at the T101 residue to form a hydrogen bond of the −OH group of T101 with heme propionate and thereby leads to the stabilization of the heme pocket in the presence of the substrate. Such a hydrogen-bond formation will however not be possible in the T101V mutant, where the −OH of threonine is replaced by $-CH_3$ of valine and, hence, the stability of the tertiary structure near the heme moiety is decreased in the T101V mutant compared to the WT enzyme in the presence of the substrate. Moreover, the replacement of threonine by valine would also not allow for the formation of any hydrogen bond with Y96, which might have some indirect role in the mechanism of camphor binding to the enzyme. Nevertheless, the absence of any such hydrogen bond because of the T101V mutation does not seem to have any effect on the camphor-binding constant nor does it affect the stability of the heme pocket in the absence of the substrate.

CONCLUSIONS

CD studies identified a small but significant change in the tertiary structure around the heme, especially in the substrate-bound cytochrome P450cam upon mutation of the T101 residue to valine. This subtle change in the tertiary structure because of the mutation did not affect the substrate-binding affinity of the enzyme.

Distinct phases of unfolding of the secondary structure and those of the various tertiary-structural elements around the active site were detected in the thermal unfolding of the WT as well as the T101V mutant of the enzyme. Although the stability of the secondary structure was found to be unaffected by the mutation, the tertiary structure around the heme became less stable in the substrate-bound enzyme upon mutation. On the other hand, the thermal stability of the substrate-free enzyme remained almost unaffected by the mutation. These results in conjunction with the reported high-resolution crystal structures of the enzyme suggested that

there might be a conformational change at the side chain of threonine 101 upon binding the substrate. This could enable the formation of a hydrogen bond between the −OH group of the threonine and one propionate group of the heme and stabilize the heme pocket in the substrate-bound enzyme. Such hydrogen bonding of the propionate group of the heme is absent in the T101V mutant, which showed a decreased stability of the tertiary structure of the heme cavity in the substrate-bound mutant enzyme.

ACKNOWLEDGMENT

The authors thank Mr. Bharat T. Kansara for assistance.

REFERENCES

1. Oritz de Montellano, P. R. (1995) *Cytochrome P450: Structure, Mechanism, and Biochemistry*, 2nd ed., Plenum Press, New York.
2. Guengerich, F. P. (1991) Reactions and significance of cytochrome P-450 enzymes, *J. Biol. Chem. 266*, 10019−10022.
3. Sono, M., Roach, M. P., Coulter, E. D., and Dawson, J. H. (1996) Heme-containing oxygenases, *Chem. Rev. 96*, 2841−2888.
4. Kellner, D. G., Maves, S. A., and Sligar, S. G. (1997) Engineering cytochrome P450s for bioremediation, *Curr. Opin. Biotechnol. 8*, 274−278.
5. Wong, L.-L. (1998) Cytochrome P450 monooxygenases, *Curr. Opin. Chem. Biol. 2*, 263−268.
6. Miles, C. S., Ost, T. W., Noble, M. A., Munro, A. W., and Chapman, S. K. (2000) Protein engineering of cytochromes P-450, *Biochim. Biophys. Acta 1543*, 383−407.
7. Mueller, E. J., Loida, P. J., and Sligar, S. G. (1995) 25 years of research on P450cam, in *Cytochrome P450: Structure, Mechanism, and Biochemistry*, 2nd ed. (Oritz de Montellano, P. R., Ed.) Plenum Press, New York.
8. Mayhew, M. P., Roitberg, A. E., Tewari, Y., Holden, M. J., Vanderah, D. J., and Vilker, V. L. (2002) Benzocycloarene hydroxylation by P450 biocatalysis, *New J. Chem. 26*, 35−42.
9. French, K. J., Rock, D. A., Manchester, J. I., Goldstein, B. M., and Jones, J. P. (2002) Active site mutations of cytochrome P450cam alter the binding, coupling, and oxidation of the foreign substrates (*R*)- and (*S*)-2-ethylhexanol, *Arch. Biochem. Biophys. 398*, 188−197.
10. Bell, S. G., Stevenson, J.-A., Boyd, H. D., Campbell, S., Riddle, A. D., Orton, E. L., and Wong, L.-L. (2002) Butane and propane oxidation by engineered cytochrome P450cam, *J. Chem. Soc., Chem. Commun.* 490−491.
11. Bell, S. G., Orton, E., Boyd, H., Stevenson, J.-A., Riddle, A., Campbell, S., and Wong, L.-L. (2003) Engineering cytochrome P450cam into an alkane hydroxylase, *J. Chem. Soc., Dalton Trans.* 2133−2140.
12. Jin, S., Makris, T. M., Bryson, T. A., Sligar, S. G., and Dawson, J. H. (2003) Epoxidation of olefins by hydroperoxo-ferric cytochrome P450, *J. Am. Chem. Soc. 125*, 3406−3407.
13. Xu, F., Bell, S. G., Lednik, J., Insley, A., Rao, Z., and Wong, L.-L. (2005) The heme monooxygenase cytochrome P450cam can be engineered to oxidize ethane to ethanol, *Angew. Chem., Int. Ed. 44*, 4029−4032.
14. Walsh, M. E., Kyritsis, P., Eady, N. A., Hill, H. A., and Wong, L.-L. (2000) Catalytic reductive dehalogenation of hexachloroethane by molecular variants of cytochrome P450cam (CYP101), *Eur. J. Biochem. 267*, 5815−5820.
15. Poulos, T. L., Finzel, B. C., and Howard, A. J. (1987) High-resolution crystal structure of cytochrome P450cam, *J. Mol. Biol. 195*, 687−700.
16. Schlichting, I., Berendzen, J., Chu, K., Stock, A. M., Maves, S. A., Benson, D. E., Sweet, R. M., Ringe, D., Petsko, G. A., and Sligar, S. G. (2000) The catalytic pathway of cytochrome P450cam at atomic resolution, *Science 287*, 1615−1622.
17. Gerber, N. C., and Sligar, S. G. (1992) Catalytic mechanism of cytochrome P-450: Evidence for a distal charge relay, *J. Am. Chem. Soc. 114*, 8742−8743.
18. Vidakovic, M., Sligar, S. G., Li, H., and Poulos, T. L. (1998) Understanding the role of the essential Asp251 in cytochrome P450cam using site-directed mutagenesis, crystallography, and kinetic solvent isotope effect, *Biochemistry 37*, 9211−9219.
19. Blobaum, A. L., Harris, D. L., and Hollenberg, P. F. (2005) P450 active site architecture and reversibility: Inactivation of cytochromes P450 2B4 and 2B4 T302A by tert-butyl acetylenes, *Biochemistry 44*, 3831−3844.
20. Imai, M., Shimada, H., Watanabe, Y., Matsushima-Hibiya, Y., Makino, R., Koga, H., Horiuchi, T., and Ishimura, Y. (1989) Uncoupling of the cytochrome P-450cam monooxygenase reaction by a single mutation, threonine-252 to alanine or valine: Possible role of the hydroxy amino acid in oxygen activation, *Proc. Natl. Acad. Sci. U.S.A. 86*, 7823−7827.
21. Nagano, S., and Poulos, T. L. (2005) Crystallographic study on the dioxygen complex of wild-type and mutant cytochrome P450cam. Implications for the dioxygen activation mechanism, *J. Biol. Chem. 280*, 31659−31663.
22. Deng, T., Macdonald, I. D., Simianu, M. C., Sykora, M., Kincaid, J. R., and Sligar, S. G. (2001) Hydrogen-bonding interactions in the active sites of cytochrome P450cam and its site-directed mutants, *J. Am. Chem. Soc. 123*, 269−278.
23. Loida, P. J., and Sligar, S. G. (1993) Molecular recognition in cytochrome P-450: Mechanism for the control of uncoupling reactions, *Biochemistry 32*, 11530−11538.
24. Sibbesen, O., Zhang, Z., and Ortiz de Montellano, P. R. (1998) Cytochrome P450cam substrate specificity: Relationship between structure and catalytic oxidation of alkylbenzenes, *Arch. Biochem. Biophys. 353*, 285−296.
25. Loida, P. J., and Sligar, S. G. (1993) Engineering cytochrome P-450cam to increase the stereospecificity and coupling of aliphatic hydroxylation, *Protein Eng. 6*, 207−212.
26. Westlake, A. C., Harford-Cross, C. F., Donovan, J., and Wong, L.-L. (1999) Mutations of glutamate-84 at the putative potassium-binding site affect camphor binding and oxidation by cytochrome P450cam, *Eur. J. Biochem. 265*, 929−935.
27. Berry, E. A., and Trumpower, B. L. (1987) Simultaneous determination of hemes a, b, and c from pyridine hemochrome spectra, *Anal. Biochem. 161*, 1−15.
28. Peterson, J. A. (1971) Camphor binding by *Pseudomonas putida* cytochrome P-450, *Arch. Biochem. Biophys. 144*, 678−693.
29. Pace, C. N. (1986) Determination and analysis of urea and guanidine hydrochloride denaturation curves, *Methods Enzymol. 131*, 266−280.
30. Murugan, R., and Mazumdar, S. (2004) Role of substrate on the conformational stability of the heme active site of cytochrome P450cam: Effect of temperature and low concentrations of denaturants, *J. Biol. Inorg. Chem. 9*, 477−488.
31. Chang, C. T., Wu, C. S., and Yang, J. T. (1978) Circular dichroic analysis of protein conformation: Inclusion of the β-turns, *Anal. Biochem. 91*, 13−31.
32. Poulos, T. L., Finzel, B. C., and Howard, A. J. (1986) Crystal structure of substrate-free *Pseudomonas putida* cytochrome P-450, *Biochemistry 25*, 5314−5322.
33. Andersson, L. A., and Peterson, J. A. (1995) Active-site analysis of ferric P450 enzymes: Hydrogen-bonding effects on the circular dichroism spectra, *Biochem. Biophys. Res. Commun. 211*, 389−395.
34. Senn, H., Keller, R. M., and Wuthrich, K. (1980) Different chirality of the axial methionine in homologous cytochromes *c* determined by ^{1}H NMR and CD spectroscopy, *Biochem. Biophys. Res. Commun. 92*, 1362−1369.
35. Santucci, R., and Ascoli, F. (1997) The Soret circular dichroism spectrum as a probe for the heme Fe(III)−Met(80) axial bond in horse cytochrome *c*, *J. Inorg. Biochem. 68*, 211−214.
36. Nolting, B., Jung, C., and Snatzke, G. (1992) Multichannel circular dichroism investigations of the structural stability of bacterial cytochrome P-450, *Biochim. Biophys. Acta 1100*, 171−176.
37. Pfeil, W., Nolting, B. O., and Jung, C. (1993) Apocytochrome P450cam is a native protein with some intermediate-like properties, *Biochemistry 32*, 8856−8862.
38. Mouro, C., Jung, C., Bondon, A., and Simonneaux, G. (1997) Comparative Fourier transform infrared studies of the secondary structure and the CO heme ligand environment in cytochrome P-450cam and cytochrome P-420cam, *Biochemistry 36*, 8125−8134.

BI060848L